



Effect of External Magnetic Field on the Efficacy of ADSC Transplantation in Rats with Spinal Cord Injury

Jiaqing XIE, Xinwen QI, Jinjin HU, Xianhong YANG, Ruoyu SONG, Shidi CHEN

The Fifth Affiliated Hospital of Zunyi Medical University, Zhuhai, China

Corresponding author: Jiaqing XIE ✉ 414326894@qq.com

ABSTRACT

AIM: To assess the effect of intravenously injected superparamagnetic iron oxide nanoparticle (SPION)-labeled adipose-derived stem cells (ADSCs) under an external magnetic field on the efficacy of ADSC transplantation in rats with spinal cord injury (SCI).

MATERIAL and METHODS: ADSCs were isolated from rats, labeled with SPIONs, and divided into magnetic and non-magnetic groups. A rat model of SCI was established, and SCI rats were randomly divided into magnetic, non-magnetic, and control groups, with ten rats in each group. Rats in the magnetic and non-magnetic groups were injected with SPION-labeled ADSCs via the tail vein. A 300-mT neodymium iron boron magnet was placed externally at the SCI site of the rats in the magnetic group. One and two weeks after successful modeling, SCI rats were scored for the degree of SCI followed by histopathology of the spinal cord, number of ADSCs at the SCI site, and growth-associated protein-43 (GAP-43) expression were determined in the spinal cord tissues.

RESULTS: One and two weeks after modeling, the Basso-beattie bresnahan (BBB) scores were the highest in the magnetic group, followed by the non-magnetic group, and the lowest in the control group. HE staining showed that the histopathological manifestations of the spinal cord in the magnetic group were somewhat improved compared to those in the non-magnetic and control groups. Two weeks after modeling, Prussian blue staining revealed that the number of ADSCs was significantly higher in the spinal cord tissue of the magnetic group than in that of the non-magnetic group. One and two weeks after modeling, western blotting revealed that the magnetic group exhibited the highest GAP-43 expression.

CONCLUSION: An external magnetic field applied at the SCI site in rats exerted a directional effect on SPION-labeled ADSCs, directing their migration and improving the efficacy of stem cell-targeted therapies for SCI.




KEYWORDS: Spinal cord injury, Mesenchymal stem cells, Magnetics, Adipose, Target




ABBREVIATIONS: SPIONs: Superparamagnetic iron oxide nanoparticles, ADSCs: Adipose-derived stem cells, SCI: Spinal cord injury, PBS: Phosphate buffered saline, BBB: Basso-beattie-bresnahan, HE: Hematoxylin-eosin staining, GAP-43: Growth-associated protein-43

INTRODUCTION

Spinal cord injury (SCI) is a central nervous system (CNS) injury caused by various pathogenic factors. A high disability rate among individuals with SCI effects substantial consequences on their families owing to the resultant loss of capacity for physical activity and self-care. Conventional

treatment methods include emergency surgical intervention for decompression, high-dose corticosteroid therapy, hyperbaric oxygen therapy, etc. These conventional approaches typically prevent or delay tissue compression and secondary damage, thereby exhibiting limited efficacy in promoting CNS injury regeneration. In recent years, continuous developments

Jiaqing XIE  : 0009-0000-6595-2262
Xinwen QI  : 0000-0001-6227-8014
Jinjin HU  : 0009-0009-6591-6582

Xianhong YANG  : 0009-0007-3875-3007
Ruoyu SONG  : 0000-0001-9202-0153
Shidi CHEN  : 0009-0008-8054-3801

in stem cell transplantation techniques have led to innovative approaches for SCI treatment, thereby providing patients with a renewed sense of optimism and novel opportunities (14,24,29,33).

Adipose-derived stem cells (ADSCs) are expected to serve as an ideal cell resource in the treatment of SCI, owing to their abundance, substantial cell extraction yields, notable capacity for differentiation, and ethical neutrality. The number of transplanted ADSCs surviving at the SCI site is a key determinant of spinal cord regeneration. Although ADSCs exhibit a certain degree of homing (34), and are capable of chemotaxis towards the SCI site, such a homing effect fails to facilitate the migration of a sufficient number of stem cells to the injury site; thus, the desired reparative effect is not achieved (12). Recent studies have shown that superparamagnetic iron-oxide nanoparticles (SPIONs) have tracer properties, superparamagnetism, and favorable biocompatibility (15). The precise treatment of stem cells can be achieved by combining SPIONs with stem cells, thereby leveraging the directed movement characteristics of SPIONs under an external magnetic field. Studies have suggested that stem cells aggregate and target specific organs or tissues when exposed to an external magnetic field (22), thereby enhancing their therapeutic effect. In this study, we intravenously injected SPION-labeled ADSCs into SCI rats under an external magnetic field and observed the effects of the external magnetic field on the migration efficiency of SPION-labeled ADSCs, restoration of neurological function in rats, and cellular morphology and protein expression.

■ MATERIAL and METHODS

This study was approved by the Ethics Committee of the Fifth Affiliated Hospital of Zunyi Medical University (Approval No. 2018-S004).

Major Reagents and Instruments

HRP goat anti-rabbit or rat IgG antibodies were purchased from Abcam (Jiangsu, China). SPIONs (30 nm; So-Fe Biomedicine, Shanghai, China). Whole protein extraction, sodium dodecyl sulfate-polyacrylamide gel electrophoresis (SDS-PAGE), enhanced chemiluminescence detection, and BCA protein quantification (KeyGEN Biotech, Jiangsu, China) kits were used. High-glucose Dulbecco's modified Eagle's medium was purchased from Gibco (Billings, MA, USA). fetal bovine serum (Gibco, Billings, USA). Type I collagenase solution (0.1%; Biocare Biotech, Hefei, China), 4% isoflurane, and 0.25% trypsin-0.04% ethylenedinitrilotetraacetic acid (Biocare Biotech).

Cell Experiments

Isolation and in vitro proliferation of rat ADSCs

A total of 37 female (Sprague) Dawley rats (12-week-old; body weight, 230 ± 23 g) were included in the study. Thirty rats were used for modeling, six were used as supplementary rats, and 1 rat was used for ADSC extraction. Rats and feed were purchased from the Guangdong Medical Experimental Animal

Center. The certificate number for the qualified experimental animals is SCXK (Yue) 2013-0002. This study was approved by the Ethics Committee of the Fifth Affiliated Hospital of Zunyi Medical University (Approval No. 2018-S004).

One healthy SD rat was randomly selected for ADSC extraction. Rats were anesthetized with 4% isoflurane. Skin preparation and sterilization were performed. Approximately 1.5 g of adipose tissue was isolated from the inguinal region, and soft tissue and small blood vessels were removed. The acquired material was rinsed using phosphate-buffered saline (PBS) until no evident blood staining was visible. Next, the adipose tissue was minced and transferred to a centrifuge tube containing 0.1% type I collagenase solution at five times the volume of the tissue. The tube was then incubated at 37°C for 45 min using a constant-temperature water bath shaker to facilitate digestion. This was followed by centrifugation and the removal of the supernatant. The pellet was resuspended in a complete culture medium, homogenized, and seeded into T25 vented cell culture flasks. The flasks were placed in a 37°C incubator with 5% CO₂ for culturing. The morphology and growth of the ADSCs were observed daily using a microscope. After 48 h, the culture medium was replaced with fresh medium. Subsequently, the culture medium was replaced every 2–3 days, considering the conditions of the culture medium and cells. Once the primary cells reached 90% confluence, they were passaged at a ratio of 1:4 in a solution of 0.25% trypsin and 0.04% ethylenedinitrilotetraacetic acid. ADSCs obtained from the third passage were used in the subsequent experiments.

Flow cytometry analysis of the surface antigens of ADSCs

The ADSCs obtained from the third passage were digested to obtain cell suspensions. Each sample was placed in an Eppendorf tube and CD29, CD44, CD14, and CD45 antibodies were sequentially added. This was followed by incubation, centrifugation, and supernatant removal. The samples were then analyzed for the expression of CD29, CD44, CD14, and CD45 on the surface of ADSCs using a flow cytometer.

Labeling ADSCs with SPIONs

A SPION suspension (1 mg/mL) and 4% poly-L-lysine were added to complete culture medium to obtain a suspension with iron at a final concentration of 25 µg/mL. The ADSCs were adjusted to obtain a cell concentration of 1×10^9 /mL. This cellular suspension was added to the culture medium containing SPIONs. Following incubation at 37°C for 24 h in a cell culture incubator, the culture medium containing the SPIONs was discarded, and the cells were washed using PBS and resuspended in regular complete culture medium.

Prussian Blue staining for determining SPION labeling efficiency

The cell slides were immersed in the culture medium containing SPION-labeled ADSCs. After 12–24 h, the ADSCs were removed once they had attached 80–90% of the slide surface. The slide surface was gently washed twice using PBS, and the cells were fixed using 4% paraformaldehyde at 25 °C for 10 min. The fixing solution was then removed and

the slides were air-dried for 15 min. The slides were rinsed twice using PBS, and then freshly prepared Prussian blue staining solution (Solution A, 2% $K_4Fe(CN)_6 \cdot 3H_2O$; Solution B, 6% HCl; equal volumes of Solution A and Solution B and let stand for 5 min) were added and allowed to stand for 30 min. The ADSCs were rinsed twice with PBS, air-dried, and stained with nuclear red for 5 min. After drying, the samples were observed and photographed using an optical microscope.

Trypan blue staining for determining the viability of SPION-labeled ADSCs

Labeled and unlabeled ADSCs were divided into five groups and placed in a CO_2 incubator. After 1, 3, and 7 days of incubation, the cells were digested and centrifuged to obtain an ADSC suspension. Next, 10 μL of 0.4% trypan blue dye was added to 90 μL of ADSC suspension using a pipette, mixed well, and transferred to a cell counting plate. After 2 min of thorough mixing, we randomly selected five fields of view under a microscope and determined the number of unstained cells (unstained cells = total cells - stained cells) and the total number of cells. Cell viability was determined using the following formula: Cell viability = (number of unstained cells/total number of cells) \times 100%.

Cell Counting Kit-8 assay for determining the proliferation ability of labeled ADSCs

Suspensions of both labeled and unlabeled ADSCs with a final cell concentration of 1×10^4 cells/mL were prepared and seeded in a 96-well plate (eight replicates, 100 μL per well). Two groups were established: the magnetic group (SPION-labeled ADSCs) and the non-magnetic group (unlabeled ADSCs). Each group was divided into three identical plates, which were prepared and placed in a CO_2 incubator. On days 1, 3, and 7, one plate was retrieved from the incubator, and 10 μL of CCK-8 reagent was added to the plate using a pipette. The plates were then incubated for 2 h. The culture plate was then removed from the incubator, the absorbance was measured at 450 nm using an enzyme-linked immunosorbent assay reader, and the optical density (OD) was determined.

Animal Experiments

Establishing a rat model of SCI

A total of 36 rats were subjected to SCI at the T10 level according to the modified Allen method described in the literature. Six rats died after the modeling procedure and were subsequently used as supplementary rats. In all the rats, the Basso, Beattie, and Bresnahan (BBB) score (3) for hind limb function was 21 before surgery. After modeling, the rats were randomly divided into magnetic, non-magnetic, and control groups, with 10 rats per group.

ADSC transplantation

For rats in the magnetic group, SPION-labeled ADSCs were digested to obtain a cell suspension with a concentration of 1×10^7 cells/mL, and the rats were injected with 0.3 mL of the cell suspension via the tail vein. A 300 mT neodymium iron boron magnet (diameter, 20 mm; thickness, 3 mm) was placed at the SCI site. The magnet was affixed using an adhesive

tape and remained in place for 14 days after surgery. For rats in the non-magnetic group, the same protocol was followed as that employed in the magnetic group, but without affixing the magnet. Rats in the control group were injected with 0.3 mL of high-glucose Dulbecco's modified Eagle's medium via the tail vein. ADSC transplantation was repeated on the second and third days.

Rat neurological function assessment

Three days, 1 week, and 2 weeks after the intervention, five rats with SCI were selected from each group for BBB score assessment. The BBB score assessment was performed by three trained researchers familiar with the process and scoring criteria. The maximum score is 21, indicating normal functioning. Researchers were blinded to the groups. The rats were allowed to move freely in an open, flat space for approximately 5 min and then observed for recovery of hind limb motor function. The score for each rat was determined by averaging the scores assigned by the three evaluators, and the group score was determined by averaging the average scores of each rat in the group.

Isolation of spinal cord tissue from the rats

One and two weeks after cell transplantation, 0.3 cm of spinal cord tissue centered at the injury site was acquired from five rats in each group. The tissue was placed in an Eppendorf tube in an ice box. Tissues were weighed, dissociated, and homogenized. Subsequently, supernatants were collected. The protein concentration was determined using a BCA protein quantification assay kit. The protein loading buffer was added and mixed thoroughly. After boiling for 10 min, the sample was briefly centrifuged and stored at $-20^\circ C$. Cardiac perfusion was performed to obtain pathological specimens of the rat spinal cord tissue. After perfusion, a 0.2-cm section of the spinal cord tissue from above and below the SCI site was acquired and fixed using 4% paraformaldehyde for subsequent histological examination.

Hematoxylin-eosin (HE) and Prussian blue staining

Rat SCI tissue samples were dehydrated, fixed, and sectioned. Rat SCI tissue samples were stained with hematoxylin and eosin HE and Prussian blue and subsequently observed under a microscope.

Western blot (WB) Analysis

The protein concentrations in the samples were determined using the BCA protein quantification method. Following SDS-PAGE, the membranes were transferred, blocked, and incubated with primary and secondary antibodies. Visualization was performed using a chemiluminescence system and the film was scanned and archived. ImageJ software version 1.8.0 (National Institutes of Health, Bethesda, MD, USA) was used to determine the density of the target bands.

Statistical Analysis

All quantitative data from this experiment are presented as mean \pm standard deviation ($\bar{x} \pm s$). An independent sample t-test was used for the statistical analysis of differences between the two groups. Analysis of variance (ANOVA) was

applied for statistical analysis of differences between the three groups and Multiple Comparisons(LSD-t) after homogeneity evaluation. Statistical significance was set at P-value < 0.05. significance. The SPSS 21 software was used for all statistical analyses.

RESULTS

Establishing a rat model of SCI

Of the 36 SD rats that were subjected to surgery, two rats in the magnetic group and 1 rat each in the non-magnetic and control groups died. Autopsy revealed that the deaths were due to inadequate vascular ligation and postoperative urinary retention-related infections. Additional rats were included to increase the number of rats in each group. The general condition of the remaining rats after surgery was favorable, with a BBB score of 0. The surgical incisions healed satisfactorily with no notable signs of exudation or infection (Figure 1).

Viability of ADSCs

The primary cells initially exhibited various morphologies, including elliptical, circular, and irregular shapes, when observed under a microscope (Figure 2A). After 12 h, most cells gradually adhered to the walls, predominantly exhibiting circular or spindle shapes. After 24 h, the majority of cells exhibited adherent growth and displayed spindle shapes (Figure 2B). After 7 days, the primary cells reached 85–90% confluency. Passaged cells exhibited an increased growth rate, achieving approximately 90% confluence within 3–5 days. The cells exhibited consistent spindle shapes after the third passage, and 90% confluence was achieved within 3 days. The cells continued to grow well even after the fifth passage, with no discernible changes in cell morphology.

Flow cytometry identification of ADSCs

Flow cytometric analysis of ADSCs obtained from the third passage showed that 50.12% of the cells expressed CD44, 44.17% expressed CD29, 0.78% expressed CD14, and 2.16% expressed CD45. These results were consistent with the general expression pattern of surface antigens on rat ADSCs. Therefore, the passaged cells were validated as ADSCs (Figure 3).

Prussian blue staining for determining the labeling rate of SPIONs

Following Prussian blue staining, we observed SPION-labeled ADSCs under a microscope and the presence of iron particles in the cytoplasm (indicated by arrows). The labeling rate was approximately 100% (Figure 4).

Trypan blue staining for determining the cell viability of labeled ADSCs

Trypan blue staining was performed on SPION-labeled ADSCs (magnetic group) and unlabeled ADSCs (non-magnetic group) on days 1, 3, and 7. There was no significant difference in cell viability between the SPION-labeled and unlabeled ADSCs ($p > 0.05$) (Table I).

CCK-8 assay for determining the proliferation ability of labeled ADSCs

A CCK-8 assay was performed to measure the OD values of the ADSCs in the magnetic and non-magnetic groups on days 1, 3, and 7. The results showed that SPION-labelled ADSCs had no significant impact on cell proliferation compared to unlabeled ADSCs ($p > 0.05$) (Table II).

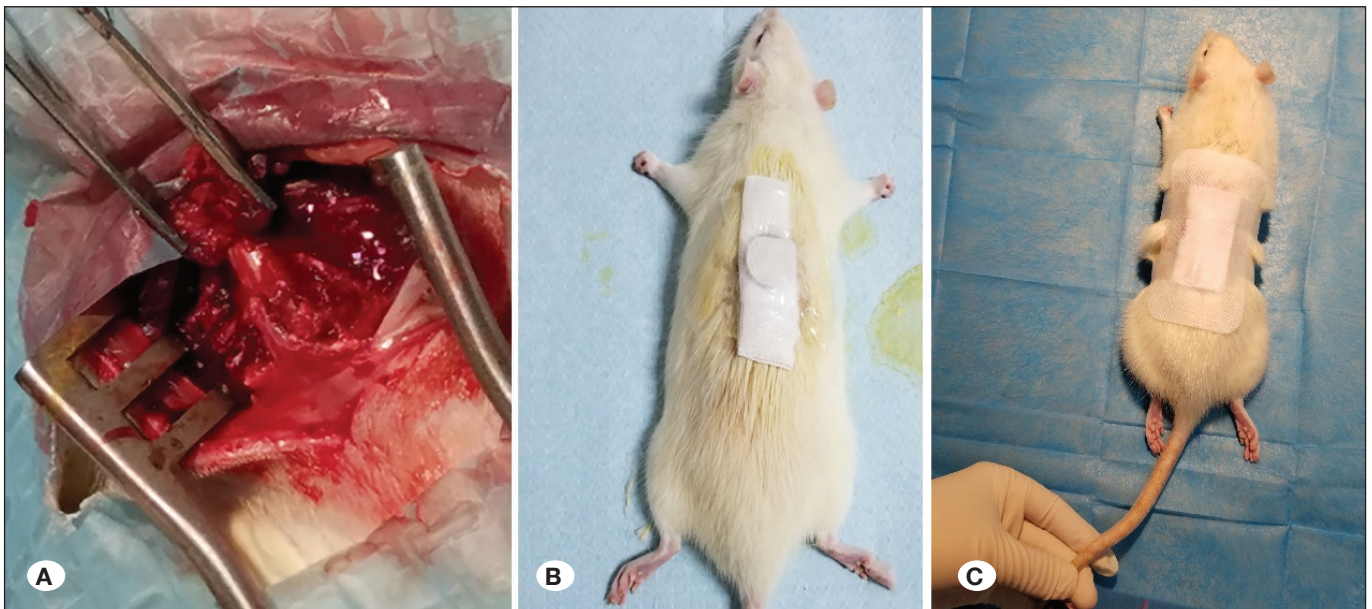


Figure 1: The general condition of the rats after modeling. **A)** Exposed spinal cord tissue during modeling; **B)** Placement of neodymium iron boron magnets at the surgical incision site and dressing. **C)** Complete paralysis of the lower limbs after recovery from anesthesia. Rats were only able to crawl using their forelimbs.

Table 1: Comparison of Cell Viability Between the Magnetic and Non-Magnetic Groups Using the Trypan Blue Staining Method (mean ± Standard Deviation, %)

Groups	Day 1	Day 3	Day 7
Magnetic group (n=5)	97.39 ± 1.35	95.99 ± 1.60	96.52 ± 1.68
Non-magnetic group (n=5)	96.61 ± 0.71	96.27 ± 1.31	97.13 ± 1.89
t	1.15	-0.30	-0.54
p-value	0.29	0.77	0.61

Note: The differences in cell viability between the magnetic and non-magnetic groups on days 1, 3, and 7 had p values >0.05, indicating no statistical significance.

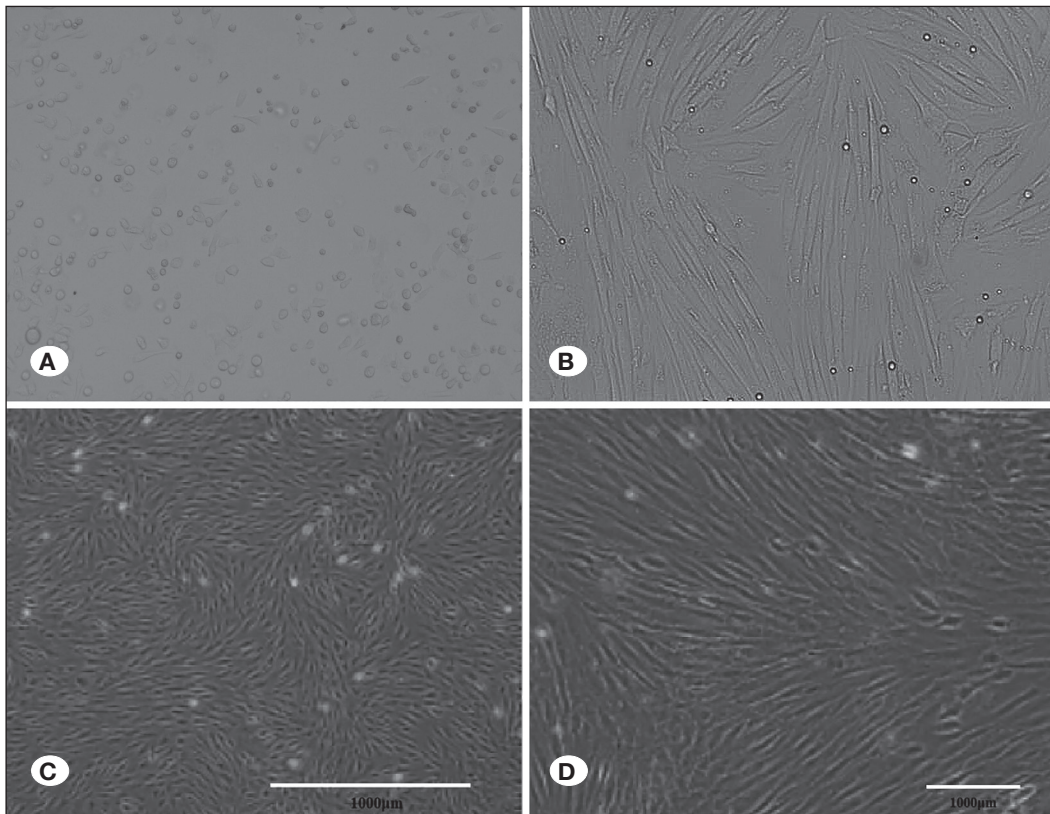


Figure 2: Culturing and passage of rat ADSCs. **A)** Primary ADSCs initially exhibited various shapes, including circular, elliptical, and irregular squares (at 40× magnification). **B)** Most primary cells were adherent and elongated after 24 h and exhibited a spindle shape. **C)** The robust growth of ADSCs obtained from the third passage are arranged in a vortex pattern. **D)** Spindle-shaped ADSCs obtained from the third passage are arranged in a radiating pattern.

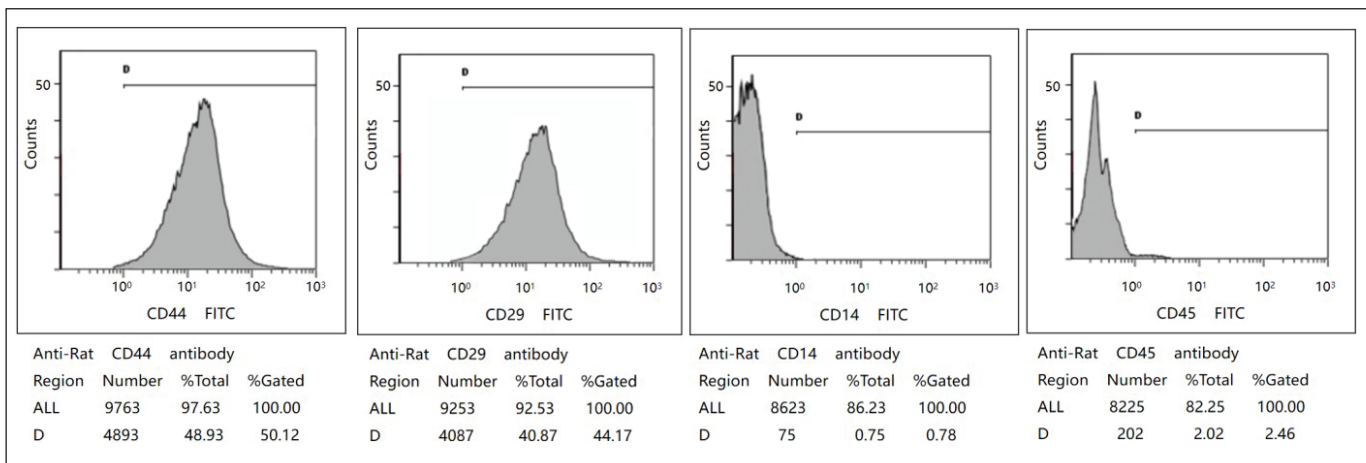


Figure 3: The results of flow cytometry were consistent with the general expression pattern of surface antigens on rat ADSCs.

Table II: OD Values in the CCK-8 Assay at Varying Time Points for the Magnetic and Non-Magnetic Groups (Mean \pm Standard Deviation)

Groups	Day 1	Day 3	Day 7
Magnetic group (n = 5)	1.24 \pm 0.05	1.28 \pm 0.03	1.42 \pm 0.06
Non-magnetic group (n = 5)	1.32 \pm 0.08	1.25 \pm 0.04	1.44 \pm 0.03
t	-2.19	1.731	-0.385
p-value	0.06	0.12	0.71

Note: The differences in cell proliferation between the magnetic and non-magnetic groups on days 1, 3, and 7 with P-values >0.05 , indicating no statistical significance.

Table III: BBB Scores at Varying Time Points After SCI in the Rats of the Three Groups (Mean \pm Standard Deviation)

Groups	Day 3	Day 7	Day 14
Magnetic group (n = 5)	3.13 \pm 0.30	5.33 \pm 0.24#*	6.33 \pm 0.53#*
Non-magnetic group (n = 5)	2.80 \pm 0.56	3.73 \pm 0.60	5.13 \pm 0.56
Control group (n = 5)	2.60 \pm 0.37	3.33 \pm 0.41	4.40 \pm 0.44#
F	2.055	29.10	18.40
p-value	0.17	0.00	0.00

Note: #Statistically significant difference compared to the non-magnetic group ($p < 0.05$). *Statistically significant difference compared to the control group ($p < 0.05$).

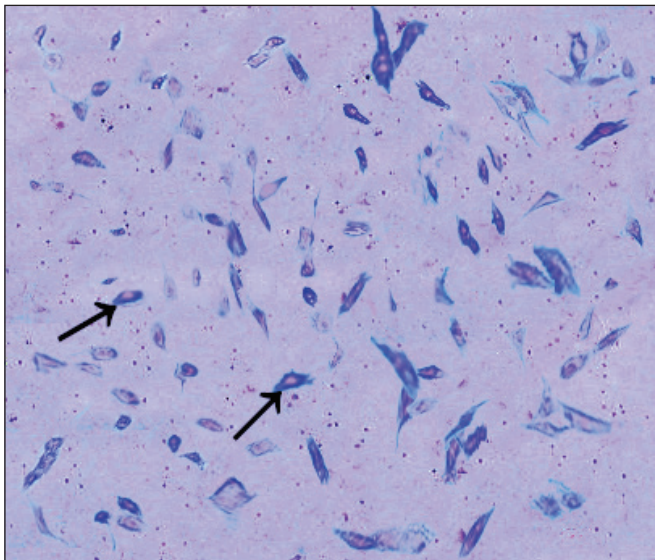


Figure 4: Prussian blue staining for determining the labeling rate of ADSCs (at 200 \times magnification).

BBB scores and comparison of SCI rats after ADSC transplantation

In all the groups, the baseline BBB scores were 21 before and 0 after modeling. No hindlimb movements were observed. On day 3 post-modeling, rats in all groups showed varying degrees of hind limb movement, with no significant differences in scores ($p > 0.05$). One week after surgery, the magnetic group showed significantly higher scores than the non-magnetic

and control groups ($p < 0.05$), whereas no significant difference in scores was observed between the non-magnetic and control groups. Two weeks after surgery, the magnetic group exhibited significantly higher scores than the non-magnetic and control groups ($p < 0.05$). Additionally, the non-magnetic group exhibited higher scores than the control group ($p < 0.05$) (Table III).

HE staining

Microscopic observation showed that one week after ADSC transplantation, rats in all groups exhibited continuous interruption of spinal cord tissue, vacuolar changes in nerve cells, formation of cavities (black arrows), and infiltration of both neural glial cells and inflammatory cells (blue arrows). The magnetic group exhibits fewer deformed and necrotic neurons and a greater number of neuronal cells with normal morphology (white arrows) than the non-magnetic and control groups. In addition, the tissues in the magnetic group exhibited favorable continuity. At two weeks, glial scars (yellow arrows) were observed at all injury sites, with the control group exhibiting the most prominent scar formation and tissue disarray (red arrows). The magnetic group exhibited the greatest number of surviving neurons, most regular tissue arrangement, and fewest glial scars (Figure 5).

Prussian blue staining

Two weeks after ADSC transplantation, we performed Prussian blue staining of the spinal cord tissues of rats in the magnetic and non-magnetic groups. The magnetic group showed a significantly higher number of blue-stained cells than the non-magnetic group (indicated by arrows) (Figure 6).

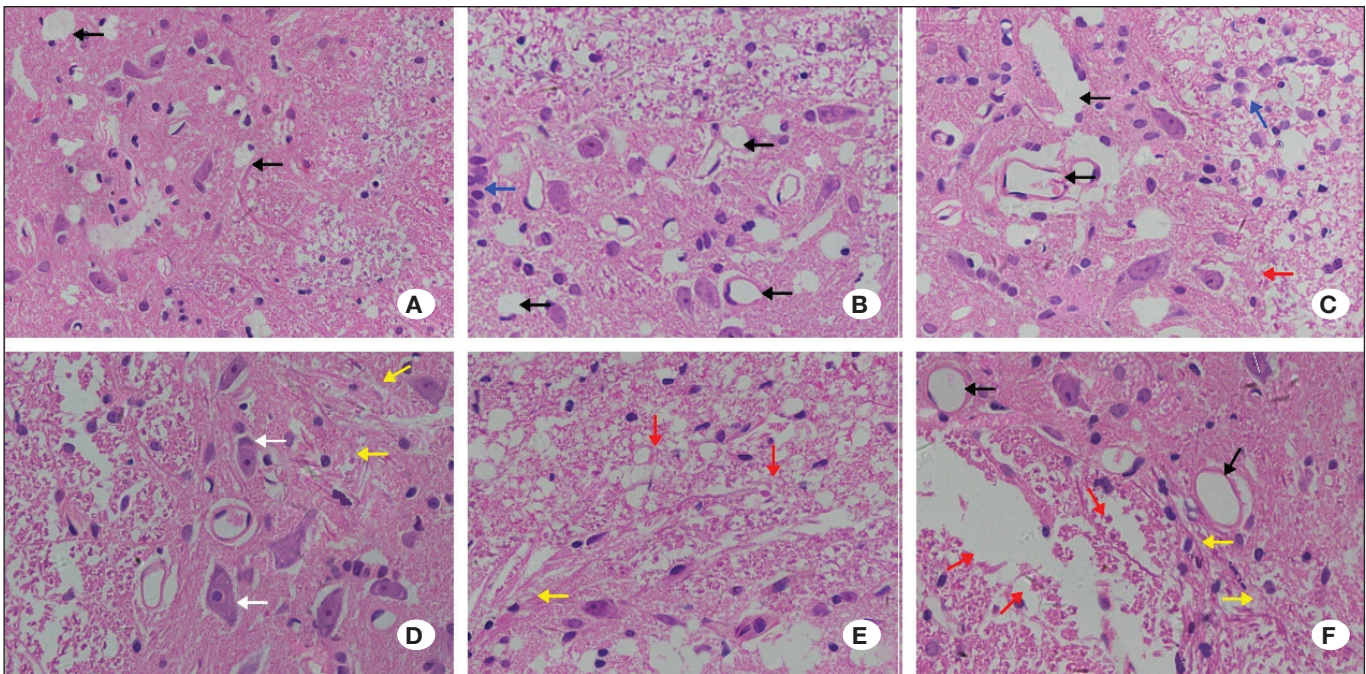


Figure 5: HE-stained sections of SCI in rats of the magnetic, non-magnetic, and control groups. **A)** One week after ADSC transplantation, the magnetic group exhibited well-organized tissue with minimal vacuolar changes in nerve cells. **B)** One week after ADSC transplantation, the non-magnetic group exhibited increased vacuolar changes in nerve cells, cavity formation, and infiltration of neural glial cells. **C)** One week after ADSC transplantation, the control group exhibited extensive vacuolar changes and disorganized tissue arrangement. **D)** Two weeks after ADSC transplantation, the magnetic group exhibited increased neuronal cell survival, normal morphology, and glial scar formation. **E)** Two weeks after ADSC transplantation, the non-magnetic group exhibited disorganized cell arrangement, decreased neuronal cells, increased formation of vacuoles, and disarrayed tissue arrangement. **F)** Two weeks after ADSC transplantation, the control group exhibited significant irregular tissue fragmentation and extensive scar formation.

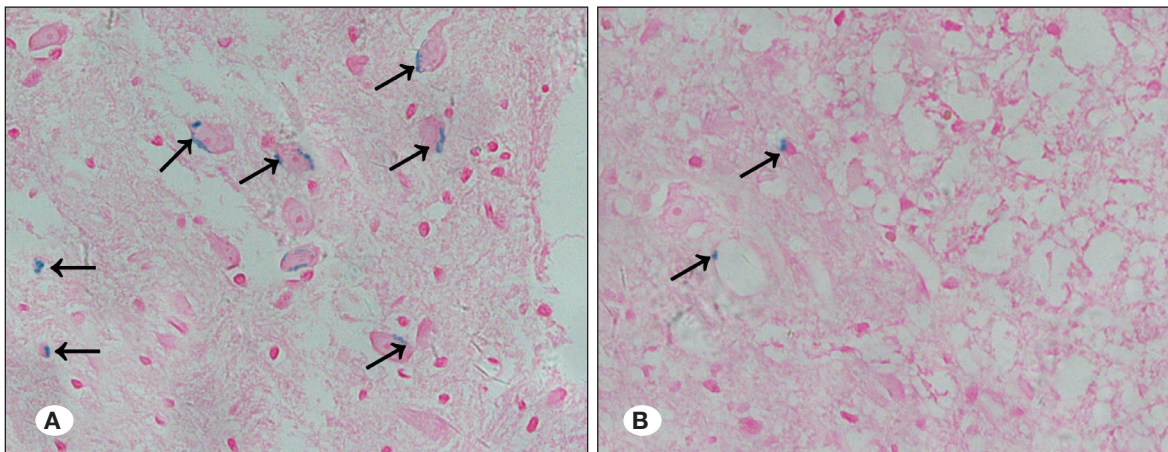


Figure 6: Detection of iron in the spinal cord tissues of rats in the magnetic and non-magnetic groups 2 weeks after ADSC transplantation. **A)** Rats in the magnetic group exhibited a higher number of blue-stained neural glia and neuronal cytoplasm than **B)** rats in the non-magnetic group.

WB analysis

Following ADSC transplantation, the protein expression of growth-associated protein-43(GAP-43) in the spinal cord tissue was determined by WB blotting. One and two weeks after ADSC transplantation, the magnetic group exhibited significantly higher protein expression of GAP-43 than the

non-magnetic and control groups ($p < 0.05$). The non-magnetic group displayed higher protein expression of GAP-43 than the control group ($p < 0.05$) (Figure 7).

DISCUSSION

At present, the primary limitation in the treatment of SCIs is

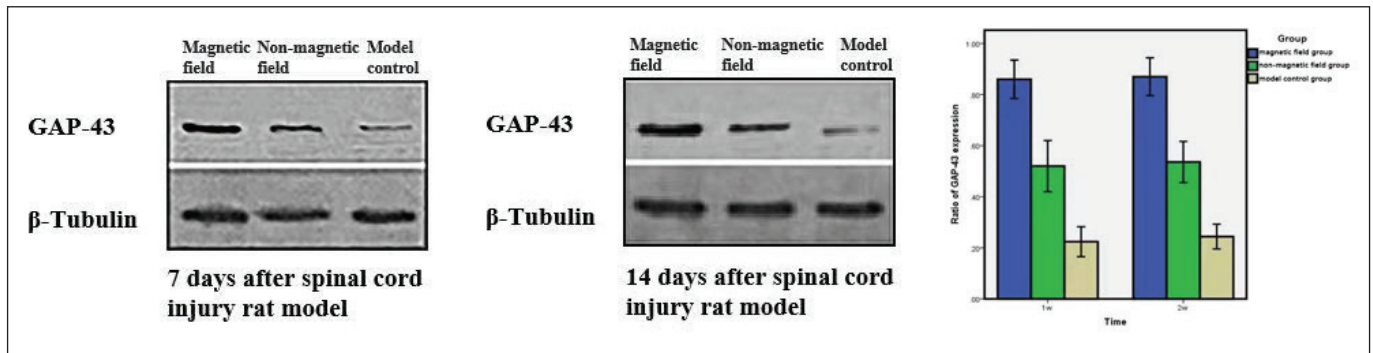


Figure 7: Quantitative detection of GAP-43 protein in the spinal cord tissue of rats in the magnetic, non-magnetic, and control groups.

the irreversible damage to CNS neurons. Clinically effective methods to promote neuronal regeneration are lacking. However, in recent years, stem cell research has shown promise for addressing this challenge (7,10,13,25). ADSCs are particularly favored by researchers because they can be easily procured in high yields (27). The administration of ADSCs via intravenous injection is a straightforward procedure with notable clinical value and has garnered considerable attention from researchers and clinicians. However, studies have revealed the inefficiency of intravenous ADSC transplantation (5,11,21), which poses challenges in effectively targeting SCI sites. Therefore, precise delivery of stem cells to the target site has emerged as a challenging task.

SPIONs are a type of magnetic nanoparticle that may be injected into the human body for use as a contrast agent for diagnostic imaging. Recent studies have shown that SPION-labelled stem cells can expeditiously migrate to target sites under the guidance of an external magnetic field (17,35). Therefore, intravenous transplantation of SPION-labeled ADSCs at the injury site under the guidance of an external magnetic field has emerged as a novel strategy for the targeted migration of stem cells. SPIONs are nanoscale particles comprising a core and coating material with properties such as superparamagnetism, low toxicity, detectability, and degradability. The particle diameter ranges from 1 to 100 nm (30,31), with the core comprising either Fe_3O_4 or $\gamma\text{-Fe}_2\text{O}_3$, both of which are natural magnets. Thus, the SPIONs are attracted to permanent magnets, which form the basis for an external magnetic field. Yang et al. used various concentrations of SPIONs to label ADSCs and revealed that a concentration of 25 $\mu\text{g}/\text{mL}$ with an incubation time of 12 h yields a labeling rate of 95% without affecting the viability and proliferation capacity of stem cells (32). This is consistent with the results of the present study, further validating the safety of SPIONs within a certain concentration range. Using a magnetic device, García-Belda elucidated that magnetically labeled cells migrate towards the center of a magnet, providing *in vitro* evidence for cell migration to the site of injury (8). In our study, ADSCs were labeled with 25 $\mu\text{g}/\text{mL}$ SPIONs, and Prussian blue staining showed a labeling rate close to 100%. Additionally, trypan blue staining and a CCK-8 assay validated that labeling ADSCs with SPION did not affect their cellular activity or proliferative capacity, demonstrating the safety of

SPIONs. Therefore, the migration and reparative effects of intravenous transplantation of SPION-labelled ADSCs in rats.

The primary objective of this study was to determine the effect of intravenous injection of magnetized ADSCs under an external magnetic field on the efficiency of ADSC transplantation in rats with SCI. The restoration of neurological function is a critical indicator of SCI repair (1). Studies have suggested that ADSCs administered intravenously at a cell density of $1 \times 10^7/\text{mL}$ can migrate to the site of SCI in rats and exert a reparative effect (19,28). These studies provided a basis for the intravenous administration dosage of ADSCs employed in the current study. The rats in the magnetic group showed varying degrees of improvement in BBB scores 1 and 2 weeks after the intravenous injection of ADSCs under an external magnetic field. This phenomenon is presumably associated with the recovery of lower-limb function in lower mammals (9). Rats in the magnetic group exhibited higher scores than those in the non-magnetic and control groups ($p < 0.05$), indicating that the degree of neurological repair may be associated with the number of ADSCs that migrate to the injury site.

The number of transplanted ADSCs surviving at the SCI site is a key factor in spinal cord repair. In one study (23), researchers placed a 380 mT neodymium magnet externally at the site of SCI in rats and subsequently injected magnetically labeled bone marrow mesenchymal stem cells (BMSCs) into the cerebrospinal fluid. The results showed a substantially greater number of BMSCs in the spinal cord of the magnetic field group than in the control group. Additional investigations (2,26) have demonstrated that externally placing neodymium magnets with magnetic field strengths of 340 and 320 mT on the liver and brain, respectively, effectively enhances the migration of neural stem cells and human mesenchymal stem cells to the site of injury. These findings are consistent with our experimental results and provide a basis for determining the optimal intensity for neodymium magnets. In this study, Prussian blue staining of spinal cord sections of rats in the three groups revealed a significantly higher number of iron-stained cells in the magnetic field group than in the non-magnetic and control groups ($p < 0.05$), indicating that the external magnetic field attracted and directed the migration of SPION-labeled ADSCs, thereby enabling a greater number of stem cells to reach the injury site.

GAP-43 is a hydrophilic protein anchored to the neuronal cell membrane. They are also involved in neuronal growth, axonal regeneration, and guidance (4,20). GAP-43 is initially expressed in neural precursor cells within the CNS (6), and plays a crucial role in neuronal and axonal development. A previous study (18) indicated that rats with a knocked-out GAP-43 gene exhibited an impaired ability to establish functional neural connections, which affects axonal regeneration and cellular structure. Following SCI, the levels of GAP-43 expression in the neuronal growth cone membrane may be 10–20-fold higher than the levels prior to injury (16), thereby influencing axonal regeneration and guidance, and ultimately affecting CNS regeneration. In this study, GAP-43 expression at the injury site was significantly higher in the magnetic field group than in the non-magnetic and control groups ($p < 0.05$), suggesting that the presence of a magnetic field enhanced the ability of ADSCs to promote neuronal regeneration and axonal growth. This can be attributed to the enhanced migration of a greater number of ADSCs to the SCI site facilitated by the external magnetic field. Consequently, the reparative effects of ADSCs on SCI were maximized.

CONCLUSION

The administration of SPION-labeled ADSCs via intravenous injection under an external magnetic field shows potential for the treatment of SCI in rats. The use of an external magnetic field efficiently directs labeled ADSCs to the injury site, offering a novel avenue for targeted ADSCs transplantation. However, additional research is necessary to determine the optimal quantity and density of SPION-labeled ADSCs at the injury site, optimal strength of the external magnetic field, and potential impact of excessive SPIONs on spinal cord tissue repair. Nevertheless, the accurate determination of the aforementioned parameters remains a key issue in stem cell-based therapies for CNS diseases.

Declarations

Funding: Guizhou Provincial Health and Family Planning Commission Science and Technology Fund Project (gzwjkj2016-1-006).

Availability of data and materials: The datasets generated and/or analyzed during the current study are available from the corresponding author by reasonable request.

Disclosure: The authors declare no conflict of interest concerning the materials or methods used in the study, or the findings specified in the article.

AUTHORSHIP CONTRIBUTION

Study conception and design: JX, XQ

Data collection: JX, JH, XY, RS, SC

Analysis and interpretation of results: JX, RS, SC

Draft manuscript preparation: JX, XQ

Critical revision of the article: XQ, JH, XY

Other (study supervision, fundings, materials, etc.): JX, JH, XY, RS, SC

All authors (JX, XQ, JH, XY, RS, SC) reviewed the results and approved the final version of the manuscript.

REFERENCES

- Ahmed RU, Alam M, Zheng YP: Experimental spinal cord injury and behavioral tests in laboratory rats. *Heliyon* 5:1-30, 2019. <https://doi.org/10.1016/j.heliyon.2019.e01324>
- Arbab AS, Jordan EK, Wilson LB, Yocum GT, Lewis BK, Frank JA: In vivo trafficking and targeted delivery of magnetically labeled stem cells. *Hum Gene Ther* 15:351-360, 2004. <https://doi.org/10.1089/104303404322959506>
- Basso DM, Beattie MS, Bresnahan JC: A sensitive and reliable locomotor rating scale for open field testing in rats. *J Neurotrauma* 12:1-21, 1995. <https://doi.org/10.1089/neu.1995.12.1>
- Chung D, Shum A, Caraveo G: GAP-43 and BASP1 in axon regeneration: Implications for the treatment of neurodegenerative diseases. *Front Cell Dev Biol* 8:1-17, 2020. <https://doi.org/10.3389/fcell.2020.567537>
- Doan HT, Van Pham P, Vu NB: Intravenous infusion of exosomes derived from human adipose tissue-derived stem cells promotes angiogenesis and muscle regeneration: An observational study in a murine acute limb ischemia model. *Adv Exp Med Biol* 769:1-16, 2023. https://doi.org/10.1007/5584_2023_769
- Esdar C, Oehrlein SA, Reinhardt S, Maelicke A, Herget T: The protein kinase C (PKC) substrate GAP-43 is already expressed in neural precursor cells, colocalizes with PKC ϵ and binds calmodulin. *Eur J Neurosci* 11:503-516, 1999. <https://doi.org/10.1046/j.1460-9568.1999.00455.x>
- Filippelli RL, Kamyabiazar S, Chang NC: Monitoring autophagy in neural stem and progenitor cells. *Methods Mol Biol* 2515:99-116, 2022. https://doi.org/10.1007/978-1-0716-2409-8_7
- García-Belda P, Prima-García H, Aliena-Valero A, Castelló-Ruiz M, Ulloa-Navas MJ, Ten-Esteve A, Martí-Bonmatí L, Salom JB, García-Verdugo JM, Gil-Perotín S: Intravenous SPION-labeled adipocyte-derived stem cells targeted to the brain by magnetic attraction in a rat stroke model: An ultrastructural insight into cell fate within the brain. *Nanomedicine* 39:102464, 2022. <https://doi.org/10.1016/j.nano.2021.102464>
- Gimenez y Ribotta M, Orsal D, Feraboli-Lohnherr D, Privat A: Recovery of locomotion following transplantation of monoaminergic neurons in the spinal cord of paraplegic rats. *Ann N Y Acad Sci* 860:393-411, 1998. <https://doi.org/10.1111/j.1749-6632.1998.tb09064.x>
- Gordon J, Amini S, White MK: General overview of neuronal cell culture. *Methods Mol Biol* 1078:1-8, 2013. https://doi.org/10.1007/978-1-62703-640-5_1
- Li G, Yu C, Yu P, Peng Q, Wang Q, Ren S, Li H, Li M, Li P, He R: Periurethral and Intravenous injections of adipose-derived stem cells to promote local tissue recovery in a rat model of stress urinary incontinence. *Urology* 167:82-89, 2022. <https://doi.org/10.1016/j.urology.2022.05.018>
- Liau LL, Looi QH, Chia WC, Subramaniam T, Ng MH, Law JX: Treatment of spinal cord injury with mesenchymal stem cells. *Cell Biosci* 10:1-17, 2020. <https://doi.org/10.1186/s13578-020-00475-3>

13. Lin HC, He Z, Ebert S, Schörnig M, Santel M, Nikolova MT, Weigert A, Hevers W, Kasri NN, Taverna E, Camp JG, Treutlein B: NGN2 induces diverse neuron types from human pluripotency. *Stem Cell Reports* 16:2118-2127, 2021. <https://doi.org/10.1016/j.stemcr.2021.07.006>
14. Liu B, Qu J, Zhang W, Izpisua Belmonte JC, Liu GH: A stem cell aging framework, from mechanisms to interventions. *Cell Rep* 41:1-16, 2022. <https://doi.org/10.1016/j.celrep.2022.111451>
15. Liu T, Wang Y, Lu L, Liu Y: SPIONs mediated magnetic actuation promotes nerve regeneration by inducing and maintaining repair-supportive phenotypes in Schwann cells. *J Nanobiotechnol* 20:159, 2022. <https://doi.org/10.1186/s12951-022-01337-5>
16. Liu W, Glueckert R, Linthicum FH, Rieger G, Blumer M, Bitsche M, Pechriggl E, Rask-Andersen H, Schrott-Fischer A: Possible role of gap junction intercellular channels and connexin 43 in satellite glial cells (SGCs) for preservation of human spiral ganglion neurons: A comparative study with clinical implications. *Cell Tissue Res* 355:267-278, 2014. <https://doi.org/10.1007/s00441-013-1735-2>
17. Meng Y, Shi C, Hu B, Gong J, Zhong X, Lin X, Zhang X, Liu J, Liu C, Xu H: External magnetic field promotes homing of magnetized stem cells following subcutaneous injection. *BMC Cell Biol* 18:24, 2017. <https://doi.org/10.1186/s12860-017-0140-1>
18. Metz GA, Schwab ME: Behavioral characterization in a comprehensive mouse test battery reveals motor and sensory impairments in growth-associated protein-43 null mutant mice. *Neuroscience* 129:563-574, 2004. <https://doi.org/10.1016/j.neuroscience.2004.07.053>
19. Min J, Kim JH, Choi KH, Yoon HH, Jeon SR: Is There additive therapeutic effect when gcsf combined with adipose-derived stem cell in a rat model of acute spinal cord injury?. *J Korean Neurosurg Soc* 60:404-416, 2017. <https://doi.org/10.3340/jkns.2016.1010.008>
20. Moradi F, Copeland EN, Baranowski RW, Scholey AE, Stuart JA, Fajardo VA: Calmodulin-binding proteins in muscle: A minireview on nuclear receptor interacting protein, neurogranin, and growth-associated protein 43. *Int J Mol Sci* 21:1-12, 2020. <https://doi.org/10.3390/ijms21031016>
21. Naeimi A, Zaminy A, Amini N, Balabandi R, Golipoor Z: Effects of melatonin-pretreated adipose-derived mesenchymal stem cells (MSC) in an animal model of spinal cord injury. *BMC Neurosci* 23:65, 2022. <https://doi.org/10.1186/s12868-022-00752-6>
22. Naseroleslami M, Aboutaleb N, Parivar K: The effects of superparamagnetic iron oxide nanoparticles-labeled mesenchymal stem cells in the presence of a magnetic field on attenuation of injury after heart failure. *Drug Deliv Transl Res* 8:1214-1225, 2018. <https://doi.org/10.1007/s13346-018-0567-8>
23. Nishida K, Tanaka N, Nakanishi K, Kamei N, Hamasaki T, Yanada S, Mochizuki Y, Ochi M: Magnetic targeting of bone marrow stromal cells into spinal cord: Through cerebrospinal fluid. *Neuroreport* 17:1269-1272, 2006. <https://doi.org/10.1097/01.wnr.0000227993.07799.a2>
24. Saba JA, Liakath-Ali K, Green R, Watt FM: Translational control of stem cell function. *Nat Rev Mol Cell Biol* 22:671-690, 2021. <https://doi.org/10.1038/s41580-021-00386-2>
25. Sivandzade F, Cucullo L: Regenerative stem cell therapy for neurodegenerative diseases: An overview. *Int J Mol Sci* 22:2153, 2021. <https://doi.org/10.3390/ijms22042153>
26. Song M, Kim YJ, Kim YH, Roh J, Kim SU, Yoon BW: Using a neodymium magnet to target delivery of ferumoxide-labeled human neural stem cells in a rat model of focal cerebral ischemia. *Hum Gene Ther* 21:603-610, 2010. <https://doi.org/10.1089/hum.2009.144>
27. Suzuki E, Fujita D, Takahashi M, Oba S, Nishimatsu H: Adipose tissue-derived stem cells as a therapeutic tool for cardiovascular disease. *World J Cardiol* 7:454-465, 2015. <https://doi.org/10.4330/wjc.v7.i8.454>
28. Tang L, Lu X, Zhu R, Qian T, Tao Y, Li K, Zheng J, Zhao P, Li S, Wang X: Adipose-derived stem cells expressing the neurogenin-2 promote functional recovery after spinal cord injury in rat. *Cell Mol Neurobiol* 36:657-667, 2016. <https://doi.org/10.1007/s10571-015-0246-y>
29. Urbán N, Cheung TH: Stem cell quiescence: The challenging path to activation. *Development* 148:1-11, 2021. <https://doi.org/10.1242/dev.165084>
30. Vangijzegem T, Stanicki D, Laurent S: Magnetic iron oxide nanoparticles for drug delivery: Applications and characteristics. *Expert Opin Drug Deliv* 16:69-78, 2019. <https://doi.org/10.1080/17425247.2019.1554647>
31. Wei H, Hu Y, Wang J, Gao X, Qian X, Tang M: Superparamagnetic iron oxide nanoparticles: Cytotoxicity, metabolism, and cellular behavior in biomedicine applications. *Int J Nanomedicine* 16:6097-6113, 2021. <https://doi.org/10.2147/IJN.S321984>
32. Yang G, Ma W, Zhang B, Xie Q: The labeling of stem cells by superparamagnetic iron oxide nanoparticles modified with PEG/PVP or PEG/PEI. *Mater Sci Eng C Mater Biol Appl* 62:384-390, 2016. <https://doi.org/10.1016/j.msec.2016.01.090>
33. Zhang L, Ma XJ, Fei YY, Han HT, Xu J, Cheng L, Li X: Stem cell therapy in liver regeneration: Focus on mesenchymal stem cells and induced pluripotent stem cells. *Pharmacol Ther* 232:108004, 2022. <https://doi.org/10.1016/j.pharmthera.2021.108004>
34. Zhao Y, Zhang H: Update on the mechanisms of homing of adipose tissue-derived stem cells. *Cytotherapy* 18:816-827, 2016. <https://doi.org/10.1016/j.jcyt.2016.04.008>
35. Zheng L, Zhang L, Chen L, Jiang J, Zhou X, Wang M, Fan Y: Static magnetic field regulates proliferation, migration, differentiation, and YAP/TAZ activation of human dental pulp stem cells. *J Tissue Eng Regen Med* 12:2029-2040, 2018. <https://doi.org/10.1002/term.2737>